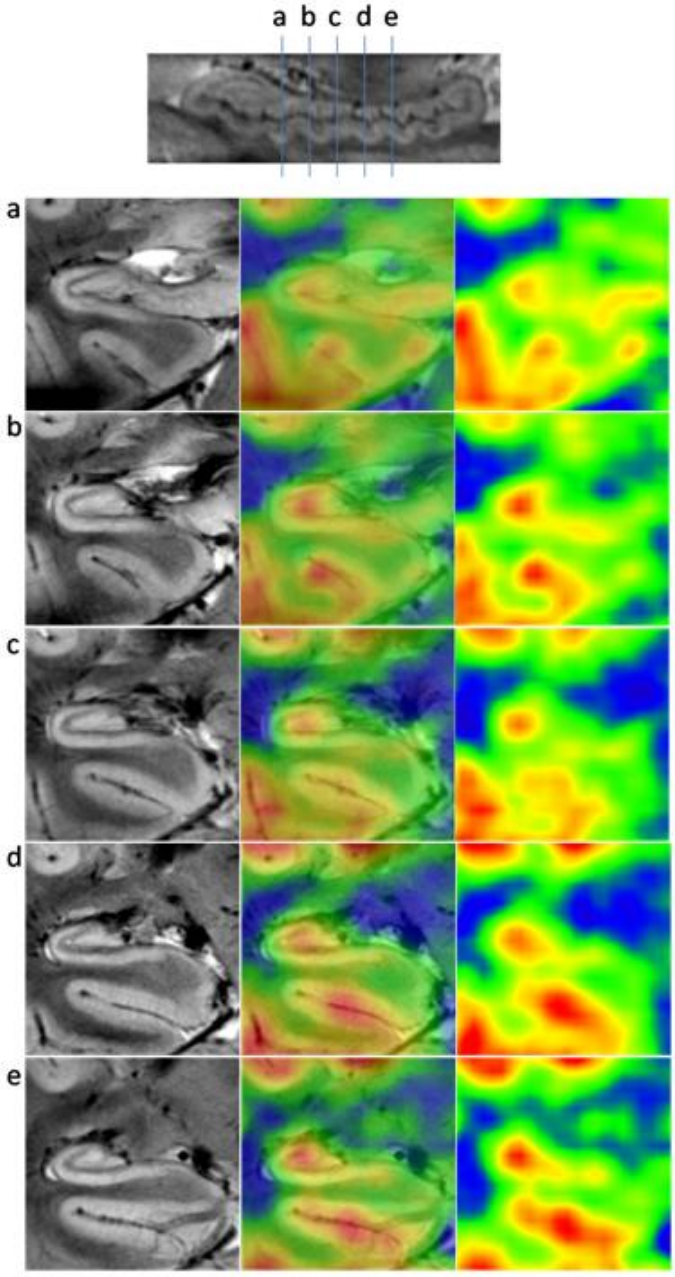

Supplemental Figure 1. An example of glucose uptake within the hippocampus of a volunteer (intra-subject data). In the left most column of images are the series of coronal sections of the left hippocampus separated with a 2.7 mm interval (**a-e**). In the middle column, corresponding PET-MRI fusion images are shown. Right most column is the set of the corresponding FDG-PET images obtained HRRT-PET. Note the varying activities of glucose metabolism within the hippocampus among the subregions. For example, CA4 regions along the slices following the hippocampal body axis, consistently show the strongest uptake among the hippocampal substructures.

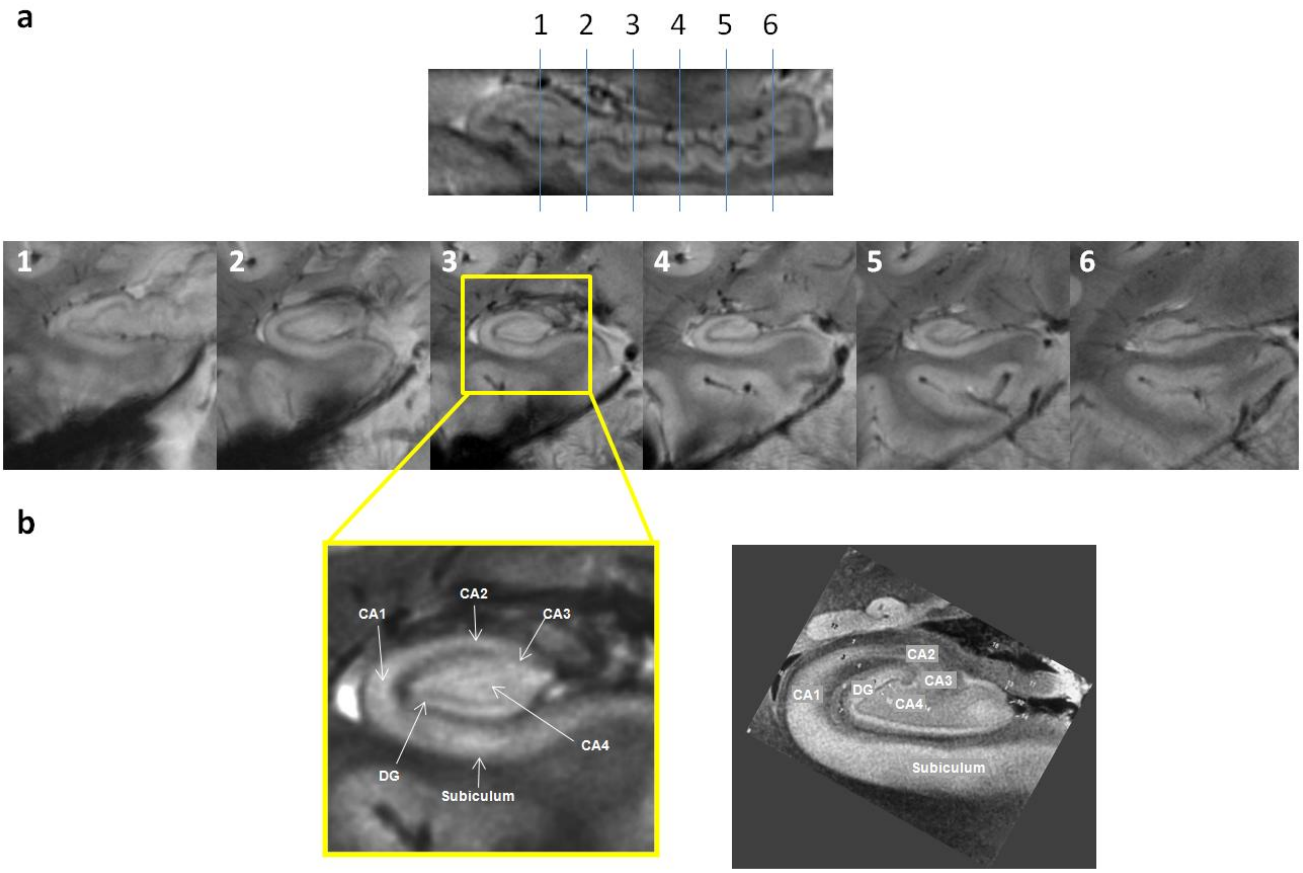

Supplemental Figure 2. In-vivo human hippocampal images obtained by the 7.0T MRI. (**a**) A series of cross-sectional images from the head to the tail of the hippocampus. As seen, the hippocampal sulcus was well defined in every slice and the important landmarks of the subregions of hippocampus are well visualized. (**b**) Magnified *in-vivo* MR image of 7.0T-MRI (left) shows good correlation with the *ex-vivo* 9.4T MR image (right) (courtesy of H. Duvernoy, Université de Franche-Comté. Reprinted with permision-of Ref. 9) of hippocampus.

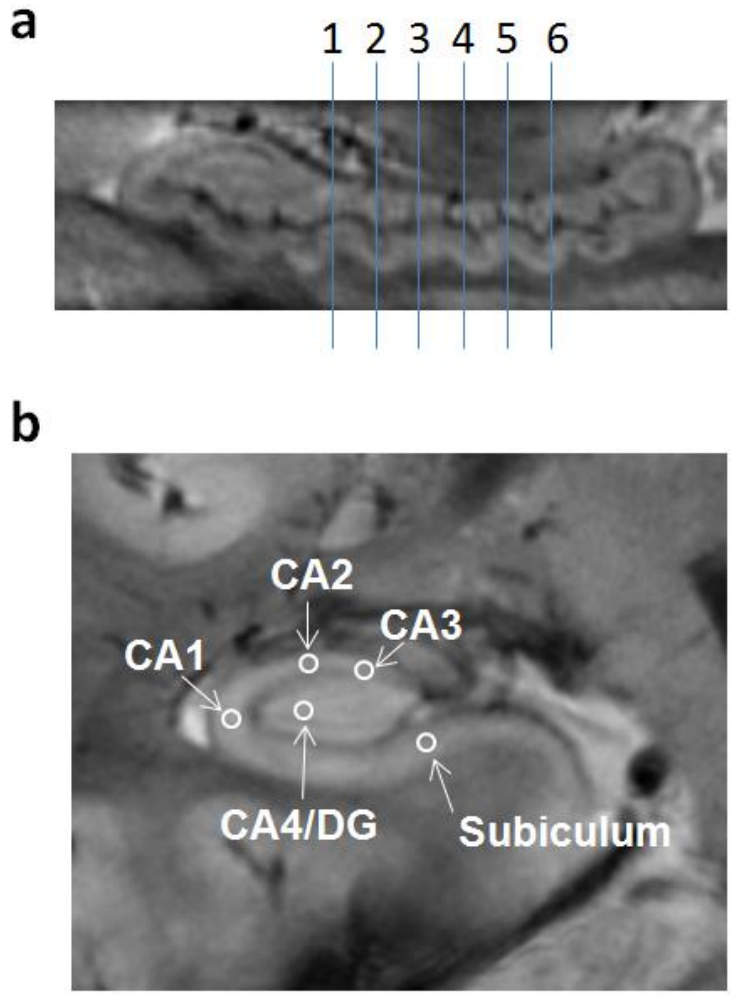

Supplemental Figure 3. ROIs for the glucose uptake measurement. (**a**) A sagittal image along the longest axis of hippocampus and the six data sampled positions of the coronal slices (blue lines) taken for the measurement of the glucose metabolism shown in the Fig. 3. The selected slices are all within the hippocampal body and excluded the head and tail part of the hippocampus. Each slice was separated about 6 mm and the similar locations were selected among the subjects by inspecting the surrounding vessel and cortical structures. (**b**) Five ROIs selected within the hippocampus for the uptake measurement. Each ROI was 1 mm diameter circle and placed in the central areas of each region.

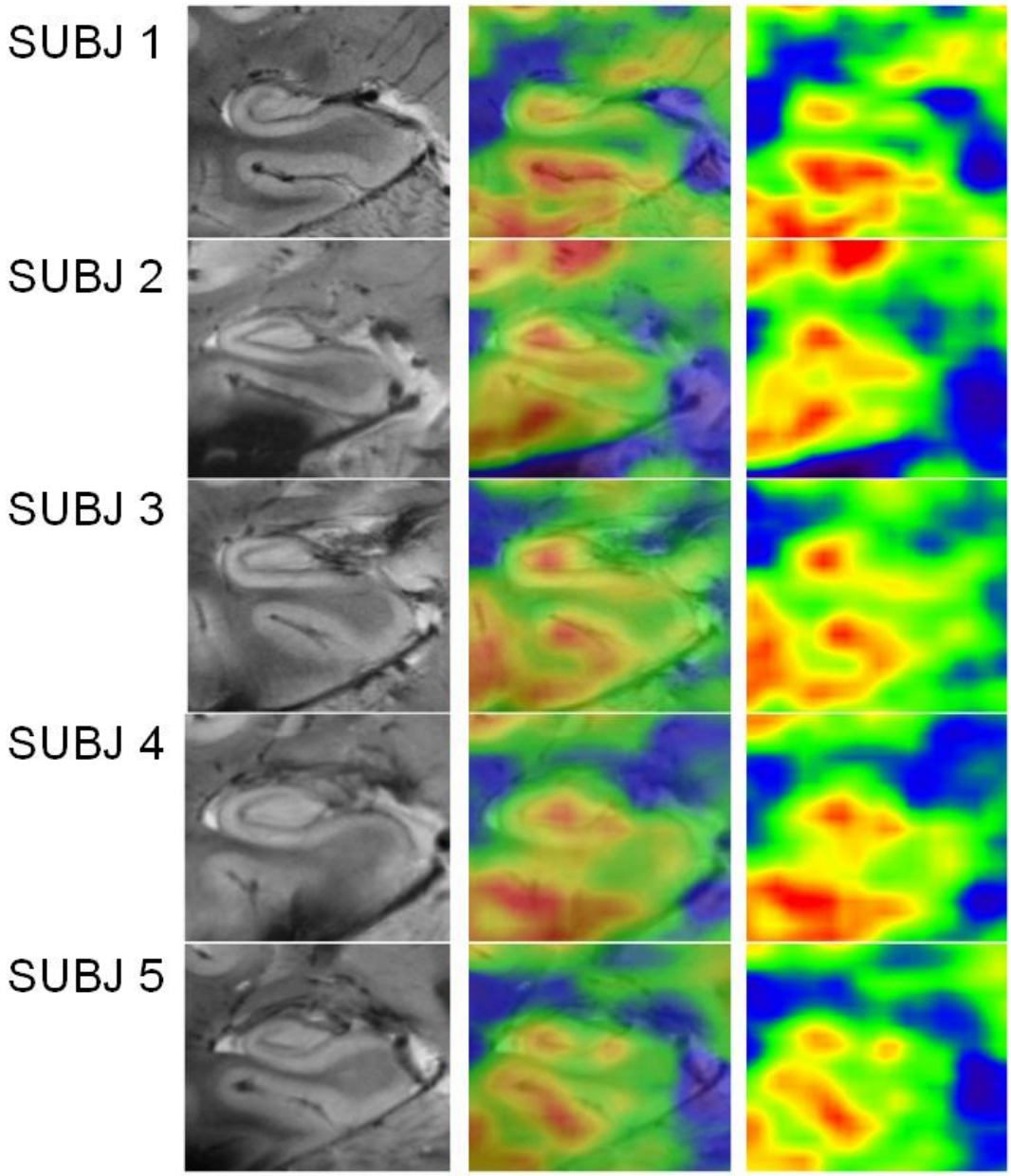

Supplemental Figure 4. Glucose metabolism of the hippocampus in five different subjects (inter-subject data).

Glucose uptake patterns were consistent among the subjects showing higher glucose metabolism in the CA4/DG region.

Supplemental Methods

Detailed description of the HRRT-PET and 7.0T-MRI fusion system can be found in the reference [11] of the manuscript. The accuracy of the system was measured using a calibration phantom. The phantom was repetitively measured for twenty times in the PET-MRI fusion system.The standard deviation of the shuttle table positioning fluctuation was ±0.08 mm, ±0.06 mm, ±0.22 mm for x, y, z translation and ±0.10 ^{o}, ±0.07 ^{o}, ±0.15 ^{o} for x, y, z rotation, respectively. The head position was automatically assigned in the two systems by our own software. The relative position was calculated and stored in the system by the precalibration process using the house-made calibration phantom.The head was immobilized as tightly as possible by the fixation foam in order to prevent movement of the subject.